STRESS-STRAIN MODEL FOR GFRP-RC CIRCULAR CONCRETE COLUMNS

Afifi, M.Z.[1], Mohamed, H. M.[1], and Benmokrane, B.[1]*
[1] Department of civil engineering, University of Sherbrooke, Sherbrooke, Quebec, Canada
* Corresponding author (Brahim.Benmokrane@Usherbrooke.ca)

Keywords*: Concrete column; GFRP bars; stress; strain; confinement model.*

ABSTRACT

The need of using glass-fiber reinforced-concrete (GFRP) as an internal reinforcement in columns increases as the deterioration problems of the conventional steel reinforcement increases. This study incorporated test results of 12 GFRP-RC columns to predict the stress–strain relationship of such columns. The results of this study can be considered as a fundamental step toward introducing a confinement model for using GFRP spirals and hoops as internal reinforcement in RC columns. New proposed equations for stress–strain relationship of concrete columns confined by GFRP spirals or hoops with various configurations are proposed. The models show good correlations with the stress–strain relationship established experimentally. Limiting GFRP hoop tensile stress to 0.004EF provided reasonable predictions for the confined concrete compressive strength of tested GFRP-RC columns, however, more experimental works are needed to validate this limit.

1 INTRODUCTION

Expansive corrosion of steel reinforcing bars stands out as a significant factor limiting the life expectancy of reinforced concrete (RC) structures. Recently, use of glass fiber-reinforced polymer (GFRP) bars as an alternative reinforcing material in RC structures has emerged as an innovative solution to the corrosion problem. GFRP composite bars in general offer many advantages over conventional steel, including one-quarter to one-fifth the density of steel, no corrosion even in harsh chemical environments, and greater tensile strength than steel.

In the past, various confinement models have been proposed for RC columns with steel reinforcement [1-4]. It has been demonstrated that suitable confinement of the concrete core with transverse reinforcement enhances both strength and ductility. In particular, strength enhancement from confinement and the slope of the descending branch of the concrete stress-strain curve has a considerable influence on the flexural strength and ductility of RC columns [4]. Since the initial studies on GFRP-confined concrete, several analytical and empirical models with varying degrees of sophistication have been suggested to predict the stress-strain response [5-12]. A number of these models evolved as extensions of the Mander et al. (1988) model [4]. In general, the elastic behavior of GFRP, unlike that of steel, provides increasing confining pressure. As the axial concrete strain increases under axial load, the confining stress continues to increase with concrete expansion until rupture of FRP due to its linear elastic-brittle properties. In contrast, in the case of steel-confined concrete, the lateral confining stress remains basically unchanged or increases insignificantly with concrete expansion after the steel has yielded. Confinement in that phase can be approximated as constant active confinement, and the overall confined concrete behavior is dominated by concrete properties [13]. Up to date, no confinement models exist in literature for circular columns reinforced with GFRP bars and confined by GFRP spirals or hoops. More experimental and theoretical studies are required to better understand the responses of rectangular and circular GFRP RC columns.

This study focused on the development of a simple design proposal to predict the stress–strain relationship for circular concrete columns reinforced with GFRP bars and confined by GFRP spirals or hoops. The results of this study can be considered as a fundamental step toward introducing a confinement model for using GFRP spirals and hoops as internal reinforcement in RC columns.

2 EXPERIMENTAL PROGRAM

2.1 Materials

In this study, 12 circular RC columns were tested under pure axial compression load. The tested columns were short columns measuring 300 mm and 1500 mm in diameter and height, respectively. The GFRP spiral, hoops, and longitudinal reinforcements were designed considering the CAN/CSA S806-12 [14] limitations for GFRP spiral reinforcement (clause 8.4.3.13): spiral reinforcement shall have a minimum diameter of 6 mm; the clear spacing between successive turns of a spiral shall not exceed 75 mm nor be less than 25 mm; and the specified volumetric ratio of spiral reinforcement was considered.

All the column specimens were cast using ready mixed concrete with an average compressive strength of 42.9 MPa (by testing ten concrete cylinders at the time of testing the column specimens). Different experimental parameters were included in the test matrix.

Sand-coated GFRP bars, spirals, and hoops were used and were assembled for the different column configurations [15], as shown in Figure 1. The tensile properties of the longitudinal GFRP bars and the transverse reinforcement were determined by performing test method B.2 and B.5 [16], respectively. Table 1 shows the mechanical properties of longitudinal GFRP bars. In addition, Table 2 presents the bent tensile strength of the transverse reinforcement $\left(f_{fu,bent} \right)$ calculated according to ACI 440.1R-15 [16].

Figure 1: Overview of the of the assembled GFRP cages.

Bar Size	d_b mm	A_F mm²	E_F GPa	f_{fu} MPa	ε_{fu} (%)
# 5	15.9	199	55.4	934	1.56

Table 1. Mechanical properties of the longitudinal GFRP bars [15]

Bar Size	Straight Portion			Bent Portion $f_{fu,bent}$ MPa
	f_{fu} MPa	E_F GPa	ε_{fu} (%)	ACI 440 [16]
# 2	938	52.5	1.90	469
# 3	889	53.4	1.89	445
# 4	941	53.6	1.70	471

Table 2. Mechanical properties of the transverse GFRP reinforcement

2.2 Overview of the experimental test results

Table 3 summarizes the experimental results of the tested specimens [17-18]. The plain control specimen did not exhibit any significant post-peak behavior but rather failed suddenly after reaching peak load. The GFRP and steel RC specimens failed in a ductile manner with the gradual spalling of the concrete cover, followed by buckling of the longitudinal bars and then rupture of the spirals or hoops. During testing, limited vertical hairline cracks started to appear at approximately 85–95% of their peak loads. After the peak load, the columns lost 10–25% of their maximum capacities due to the sudden spalling of the concrete cover, with the average measured axial concrete strains ranging from 0.0020 to 0.0026. Figure 2 provides a close-up of the rupture of the GFRP spirals and hoops, as well as the buckling and rupture of the longitudinal GFRP bars. All of the columns initially behaved similarly and exhibited relatively linear load–strain behavior in the ascending part up to their peak loads. The peak load and corresponding axial strain varied somewhat, depending on the core concrete's confinement characteristics. The higher loads correspond to well-confined specimens.

Specimen	ρ_s %	ρ_{st} %	ρ_{cc} %	P_{max} (kN)	ε_{cc} ($x10^{-6}$)	f'_{cc} MPa
Plain	--	--	--	2468	--	--
S6V-3H80	1.7	1.6	2.56	3177	3050	57.3
G8V-3H80	2.2	1.5	3.51	2920	3000	55.2
G4V-3H80	1.1	1.5	1.75	2826	2755	49.2
G12V-3H80	3.2	1.5	5.26	2998	3170	56.3
G8V-2H80	2.2	0.7	3.41	2857	2500	47.8
G8V-4H80	2.2	2.7	3.60	3019	3501	56.8
G8V-3H40	2.2	3.0	3.51	2964	5190	60.2
G8V-3H120	2.2	1.0	3.51	2804	2750	47.7
G8V-2H35	2.2	1.5	3.41	2951	4046	61.5
G8V-4H145	2.2	1.5	3.60	2865	2750	49.8
G8V-3O200	2.2	1.5	3.51	2840	2651	51.4
G8V-3O400	2.2	1.5	3.51	2871	2751	51.8
G8V-3O600	2.2	1.5	3.51	2935	2900	52.6

Table 3. Test matrix, specimens' details and experimental results

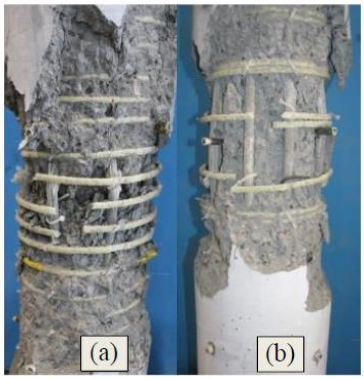

Figure 2: Close-up view of the test region showing buckling of the longitudinal GFRP bars and rupture of the (a) spirals and (b) hoops.

3 THEORETICAL INVESTIGATION

3.1 Development of stress–strain relationship

Reinforced-concrete columns subjected to axial compression load exhibit lateral expansion due to Poisson's effect up to the rupture of the transverse reinforcement. In general, large higher axial compressive strains in the column require a greater amount of confining reinforcement to achieve ductile performance. Test results of the dilation and volumetric strain behavior of the tested GFRP RC columns clearly indicated that the confinement produced by GFRP spirals or hoops led to an enhancement of ductility and confinement effectiveness. In the concrete columns confined with steel ties, spirals, or hoops, the lateral confining stress remained basically unchanged or increased insignificantly with expansion of concrete after the yielding of the steel [13], since FRP reinforcing bars behave in a linearly elastic manner up to failure. This is not the case with the concrete columns reinforced with FRP reinforcement. Moreover, the results of analysis herein show that the steel-based model (such as Mander et al. [4]) does not sufficiently reflect the behavior of GFRP RC columns.

Modeling of the stress–strain relationship is necessary for analysis and design in order to assess the deformability and ductility of concrete columns. This analysis required an analytical stress–strain relationship model of concrete in compression for both the confined and unconfined states. In this study, a general mathematical model was developed to describe the stress–strain ($f_c - \varepsilon_c$) relationship in circular GFRP RC columns. The relationship accounts for the main parameters that influence the stress–strain response such as; amount of longitudinal reinforcement, transverse-reinforcement configuration, volumetric ratio of trans- verse reinforcement to concrete core, and the mechanical properties of longitudinal and transverse reinforcements. Figure 3 shows the proposed stress–strain curve for GFRP RC columns. The curve consists of two branches: an ascending branch (pre-peak zone) and a descending branch (post-peak zone). The modification is based on experimental findings, which represent the potential of empirical and semi-empirical formulations. The proposed stress– strain relationship needed to construct the two branches of GFRP RC columns is described below.

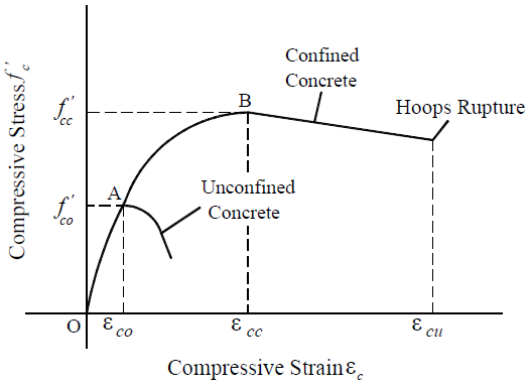

Figure 3: Schematic of the confinement stress–strain relationship.

3.1.1 Ascending branch

In the case of monotonic compression loading, the ascending branch has small confining effects, which are negligible due to the passive confinement of transverse reinforcement and small transverse strain. Therefore, it is acceptable to use an existing confined steel-based stress–strain model for GFRP RC columns for the ascending branch. A number of stress–strain models were proposed in the last decade. In 2001, Bing et al. [19] proposed a more detailed curve to simulate the stress–strain relationship ($f_c - \varepsilon_c$). The proposed curve divided the ascending branch into two zones. The first zone OA (see Figure 3) is prior to reaching f'_{co}, considering the uncracked concrete cross section and neglecting the reinforcement's contribution. The second zone beyond f'_{co} (Zone AB in Figure 3) is where the confining restraint provided by the spirals is activated and the column is again able to carry increased load until the concrete core reaches its maximum stress f'_{cc}. In this study, the Bing et al. [19] model was adopted for the ascending part of the proposed stress–strain relationship of the GFRP confined concrete as follows:

For $0 \le \varepsilon_c \le \varepsilon_{co}$:

$$f_c = E_c \varepsilon_c + \frac{\left(f'_{co} - E_c \varepsilon_{co}\right)}{\varepsilon_{co}^{\,2}} \varepsilon_c^{\,2}$$

For $\varepsilon_{co} < \varepsilon_c \le \varepsilon_{cc}$:

$$f_c = f'_{cc} - \frac{\left(f'_{cc} - f'_{co}\right)}{\left(\varepsilon_{cc} - \varepsilon_{co}\right)^2} \left(\varepsilon_c - \varepsilon_{cc}\right)^2$$

$$\frac{f'_{cc}}{f'_{co}} = 1.0 + 4.547 \left(\frac{f'_l}{f'_{co}} \right)^{0.723}$$

$$\varepsilon_{cc} = \varepsilon_{co} + 0.024 \left(\frac{f'_l}{f'_{co}} \right)^{0.907}$$

where f'_{cc} is the compressive strength of the confined concrete and ε_{cc} is the concrete strain corresponding to f'_{cc}, and E_c is the modulus of elasticity of the concrete equal to $4,500\sqrt{f'_{co}}$ MPa [20].

3.1.2 Descending branch

Because of the complicated characteristics of the descending branch, which is controlled independently, it is easier to adjust the stress–strain model curve with experimental results. Based on the regression analysis of the test results obtained in this study, the Fafitis and Shah [21] model was adopted and modified to represent the descending part of GFRP RC columns as follows:

For $\varepsilon_{cc} \le \varepsilon_c \le \varepsilon_{cu}$:

$$f_c = f'_{cc}.\exp\left[a^*\left(\varepsilon_c - \varepsilon_{cc}\right)^b\right]$$

$$a^* = a_o^* \varepsilon_{cc}^{\ b^*}$$

$$b = a_1^* + a_2^*\left(f_l^{'} / f'_{co}\right)^{a_3^*}$$

where a_o^*; a_1^*; a_2^*, and a_3^* are constants that can be determined from experimental results. Fafitis and Shah [21] proposed $a^* = \ln 0.5\varepsilon_{cc}^{b^*}$ and $b = 0.58 + 16\left(f_l^{'} / f'_{co}\right)^{1.4}$. Interpolation of the experimental results from the GFRP RC specimens tested in this study yielded these constants:

$$a^* = -0.075\varepsilon_{cc}^{\ b^*},\ b = 24.06 - 23.72\left(f_l^{'} / f'_{co}\right)^{0.011}$$

The following equation is proposed for ε_{cu} (the maximum concrete strain) based on regression analysis of the test results from this study and adopting the Bing et al. [19] equation form:

$$\varepsilon_{cu} = \varepsilon_{co}\left[0.63 + \left(70.6 - 1.76 f'_{co}\right)\sqrt{\frac{f_l^{'}}{f'_{co}}}\right]$$

Figure 4 shows the comparisons of the experimental and analytical curves for the tested specimens. The compared test results cover a wide range of the volumetric ratio of GFRP spiral reinforcements. These values ranged from 0.7% to 2.5%. It was found that, in the case of well-confined concrete, a^* and b^* are large and produce a smooth convex falling branch. On the other hand, in the case of poorly confined concrete, a^* and b^* are small and produce a steep concave falling branch. In general, the comparisons indicate satisfactory correlation between the theoretical and experimental stress–strain relationship for the GFRP RC columns. An insignificant deviation was observed on the stress–strain relationship between the experimental and theoretical results at stage $\varepsilon_{co} < \varepsilon_c \le \varepsilon_{cc}$. This difference could be attributed to the irregular post-peak softening response and the difference in the rate of cover spalling for each specimen as resulted from the investigated test parameters. Also, at this stage the columns were susceptible to eccentric loading due to the unsymmetrical axial deformation.

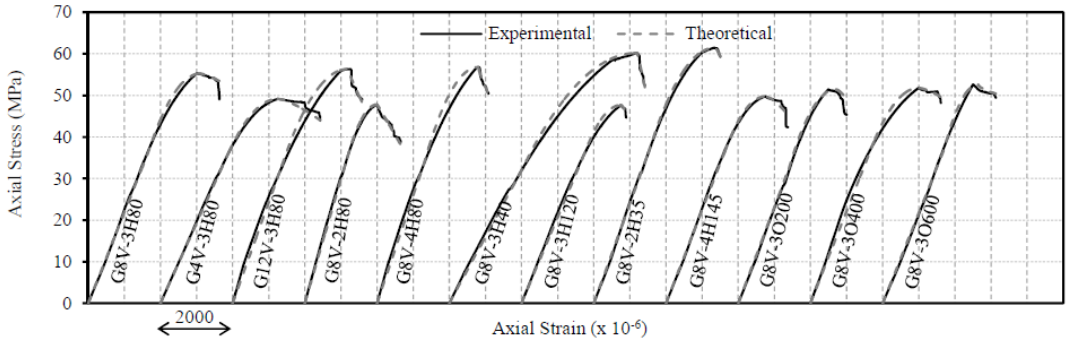

Figure 4: Experimental versus proposed stress–strain curves of the GFRP RC specimens.

4 CONCLISIONS

This study is part of an ongoing research program at the University of Sherbrooke that aims to investigate the structural performance of FRP-RC columns. This paper presented tests that were performed to investigate the compression behavior of circular concrete columns reinforced longitudinally with GFRP bars and transversely with newly developed GFRP spiral and hoops. A total of 12 full-scale RC columns were prepared to study five test variables: reinforcement type (GFRP versus steel), longitudinal FRP reinforcement ratio, and different volumetric ratios, diameters, and spacing of spiral reinforcement. This paper attempts to provide a basis for theoretical development of stress-strain behavior for concrete columns reinforced with GFRP bars and confined with GFRP spirals and hoops that can be effectively used for design purposes. Based on the experimental test results and analysis presented in this paper, the following conclusions can be drawn.

1. The experimental evidence presented in this paper indicates that the use of GFRP spirals and hoops as lateral reinforcement in accordance with CSA S806-12 (CSA 2012) limitations effectively confined the concrete core in the post-peak stages;
2. Limiting GFRP hoop tensile stress to 0.004 E_{lf} leads to conservative predictions for the confined concrete compressive strength of GFRP-RC columns.;
3. New proposed equations for the stress-strain relationship of concrete columns confined by CFRP spirals or hoops with various configurations have been proposed. The equations show good correlations with stress-strain relationships established experimentally.

5 ACKNOWLEDGMENTS

The authors would like to express their special thanks and gratitude to the Ministère de l'Économie, de l'Innovation et des Exportations of Quebec, the Natural Science and Engineering Research Council of Canada (NSERC), the Fonds de recherche du Québec—Nature et Technologies (FQRNT), Pultrall Inc. (Thetford Mines, Quebec), the Canadian Foundation for Innovation (FCI), and the technical staff of the structural lab of the Department of Civil Engineering at the University of Sherbrooke.

6 REFERENCES

[1] Richart FE, Brandtzaeg A, Brown RL. “A study of the failure of concrete under combined compressive stresses.” Engineering Experiment Station, Bulletin No. 185. Urbana: University of Illinois; 1928. 104 p.
[2] Sheikh SA, Uzmeri SM. “Strength and ductility of tied concrete columns.” J Struct Div, ASCE 1980;106(5):1079–102.
[3] Park R, Priestly MJN, Gill WD. “Ductility of square confined concrete columns.” J Struct Div, ASCE 1982;108(4):929–50.
[4] Mander JB, Priestley JN, Park R. “Theoretical stress–strain model for confined concrete.” J Struct Eng, ASCE 1988;114(8):1804–26.
[5] Fardis MN, Khalili HH. “FRP-encased concrete as a structural material.” Mag Concr Res 1982;34(121):191–202.
[6] Mirmiran A, Shahawy M. “Behavior of concrete columns confined by fiber composites.” J Struct Eng, ASCE 1997;123(5):583–90.
[7] Samaan M, Mirmiran A, Shahawy M. “Model of concrete confined by fiber composites.” J Struct Eng, ASCE 1998;124(90):1025–31.
[8] Spoelstra MR, Monti G. “FRP-confined concrete model.” J Compos Constr, ASCE 1999;3(3):143–50.
[9] Xiao Y, Wu H. “Compressive behavior of concrete confined by carbon fiber composite jackets.” J Mater Civil Eng, ASCE 2000;12(2):139–46.

[10] Lam L, Teng JG. “Strength models for fiber-reinforced plastic-confined concrete.” J Struct Eng, ASCE 2002;128(5):612–623.
[11] Jiang T, Teng JG. “Analysis-oriented stress–strain models for FRP-confined concrete.” Eng Struct 2007;29(11):2968–86.
[12] Mohamed H, Masmoudi R. “Axial load capacity of reinforced concrete-filled FRP tubes columns: experimental versus theoretical predictions.” J Compos Constr, ASCE 2010;14(2):231–43.
[13] Cui C, Sheikh SA. “Experimental study of normal- and high-strength concrete confined with fiber-reinforced polymers.” J Compos Constr, ASCE 2010;14 (5):553–61.
[14] Canadian Standards Association (CSA). “*Design and construction of building components with fiber reinforced polymers.*” CAN/CSAS806-12, Rexdale, Ontario, Canada, 2012.
[15] Pultrall Inc. Composite reinforcing rods technical data sheet. Thetford Mines, Canada; 2012. www.pultrall.com.
[16] American Concrete Institute (ACI) Committee 440. “*Guide for the design and construction of concrete reinforced with FRP bars.*” ACI 440.1R-15, Farmington Hills, MI., 2015.
[17] Afifi MZ, Mohamed HM, Benmokrane B. “Axial capacity of circular concrete columns reinforced with glass-FRP bars and spirals.” J Compos Constr, ASCE 2014;18(1):04013017.1–04013017.11.
[18] Mohamed HM, Benmokrane B. “Design and performance of reinforced concrete water chlorination tank totally reinforced with GFRP bars.” ASCE J Compos Constr 2014;18(1):05013001-1–05013001-11.
[19] Bing L, Park R, Tanaka H. “Stress–strain behavior of high-strength concrete confined by ultra-high- and normal-strength transverse reinforcements.” ACI Struct J 2001;98(3):395–406.
[20] Tikka T, Francis M, Teng B. “Strength of concrete beam columns reinforced with GFRP bars.” 2nd International structures specialty conference, Winnipeg, Manitoba, June 9–12; 2010. p. 46.1–46.10.
[21] Fafitis A, Shah SP. “Predictions of ultimate behavior of confined concrete columns subjected to large deformations.” ACI J Proc 1985;82(4): 423–33.